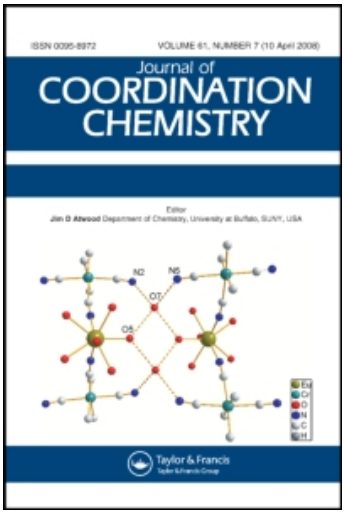

Journal of Coordination Chemistry
Publication details, including instructions for authors and subscription information:
http://www.informaworld.com/smpp/title~content=t713455674

Synthesis, crystal and spectroscopic characterization of [RuHCl(CO)(PPh_3)$_2$(pyrazine)]

J. G. MaŁecki[a]; R. Kruszynski[b]
[a] Department of Inorganic and Coordination Chemistry, Institute of Chemistry, University of Silesia, 40-006 Katowice, Poland [b] X-Ray Crystallography Laboratory, Institute of General and Ecological Chemistry, Technical University of Łódź, 90-924 Łódź, Poland

First published on: 07 June 2007

To cite this Article MaŁecki, J. G. and Kruszynski, R.(2007) 'Synthesis, crystal and spectroscopic characterization of [RuHCl(CO)(PPh_3)$_2$(pyrazine)]', Journal of Coordination Chemistry, 60: 19, 2085 — 2095, First published on: 07 June 2007 (iFirst)
To link to this Article: DOI: 10.1080/00958970701239580
URL: http://dx.doi.org/10.1080/00958970701239580

Journal of Coordination Chemistry
Vol. 60, No. 19, 1 October 2007, 2085–2095

Taylor & Francis
Taylor & Francis Group

Synthesis, crystal and spectroscopic characterization of $[RuHCl(CO)(PPh_3)_2(pyrazine)]$

J. G. MAŁECKI*† and R. KRUSZYNSKI‡

†Department of Inorganic and Coordination Chemistry, Institute of Chemistry, University of Silesia, 9th Szkolna St., 40-006 Katowice, Poland
‡X-Ray Crystallography Laboratory, Institute of General and Ecological Chemistry, Technical University of Łódź, 116 Żeromski St., 90-924 Łódź, Poland

(*Received 17 November 2005; in final form 12 January 2007*)

The reaction of $[RuHCl(CO)(PPh_3)_3]$ with pyrazine has been examined and a ruthenium(II) complex – $[RuHCl(CO)(PPh_3)_2(C_4H_4N_2)]$ – has been obtained. The compound has been studied by IR, UV–Vis spectroscopy, and X-ray crystallography. The molecular orbital diagram of the complex has been calculated with density functional theory (DFT). The spin-allowed singlet–singlet electronic transitions of the complex have been calculated with the time-dependent DFT method, and the UV–Vis spectrum of the compound has been discussed on this basis.

Keywords: Ruthenium hydrido carbonyl complexes; Pyrazine; X-ray structure; UV–Vis spectra; DFT calculations

1. Introduction

Metal complexes with pyrazine ligand are an interesting topic because pyrazine is a potential binding ligand. These types of complexes might be used as building blocks for the constructions of polynuclear architectures [1–5]. Due to the character of the pyrazine ring, containing a highly delocalized electron system with two reactive sites, the ruthenium complexes containing pyrazine have been thoroughly studied. Their electrochemical and photochemical properties [6–10], and catalytic efficiency [11, 12] were examined.

Here, we present the synthesis, crystal, molecular and electronic structure of the $[RuHCl(CO)(PPh_3)_2(C_4H_4N_2)]$.

The molecular orbital diagram of the examined complex has been calculated with the density functional theory (DFT), and additional information about binding has been obtained by NBO analysis. Density functional theory is commonly used to examine the electronic structure of transition metal complexes. It is accurate, easy to use and fast enough to allow the study of relatively large transition metal complexes [13]. The spin-allowed singlet–singlet electronic transitions of $[RuHCl(CO)(PPh_3)_2(C_4H_4N_2)]$ have

*Corresponding author. Email: gmalecki@us.edu.pl

ISSN 0095-8972 print/ISSN 1029-0389 online © 2007 Taylor & Francis
DOI: 10.1080/00958970701239580

been calculated with time-dependent DFT (TDDFT method), and a good agreement with the experimental spectrum has been observed.

2. Experimental

2.1. *Physical measurements*

Infrared spectra were recorded on a Nicolet Magna 560 spectrophotometer in the spectral range 4000–400 cm^{-1} using KBr pellets. Electronic spectra were measured on a Lab Alliance UV–Vis 8500 spectrophotometer in the range of 800–200 nm in dichloromethane. Elemental analyses (C, H, N) were performed on a Perkin–Elemer CHN-2400 analyzer. The ^1H NMR spectrum was obtained at room temperature in $CDCl_3$ using an INOVA 300 spectrometer.

All reagents used for the synthesis of the complex are commercially available and were used without further purification. The $[RuHCl(CO)(PPh_3)_3]$ complex was synthesized using a literature method [14].

2.2. *Synthesis of $[RuHCl(CO)(PPh_3)_2(C_4H_4N_2)]$*

A suspension of $[RuHCl(CO)(PPh_3)_3]$ (0.95 g; 1×10^{-3} mol) and pyrazine (0.16 g; 2×10^{-3} mol) in methanol (100 cm^{-3}) was refluxed until the solid dissolved, then was cooled and filtered. Orange crystals suitable for X-ray crystal analysis were obtained by slow evaporation of the reaction mixture. Yield 81%. Anal. Calcd for $C_{41}H_{35}ClN_2OP_2Ru$: C 63.94%; H 4.58%; Cl 4.60%; N 3.64%; P 8.4%; Ru 13.12%. Found: C 64.01%; H 4.53%; N 3.66%.

IR (KBr): 3052 $\nu_{CH-pyrazine}$; 3021 $\nu_{CH-phenyl}$; 2005 ν_{Ru-H}; 1932 ν_{CO}; 1586 ν_{CN}; 1480 $\delta_{(C-CH\ in\ the\ plane)}$; 1433 $\nu_{Ph(P-Ph)}$; 1093 $\delta_{(C-CH\ in\ the\ plane)}$; 997 $\delta_{(C-C\ out\ of\ the\ plane)}$; 747 $\delta_{(C-C\ out\ of\ the\ plane)}$; 696 $\delta_{(C-C\ in\ the\ plane)}$; 608 ν_{P-Ph}. ^1H NMR (δ, $CDCl_3$): −13.55 (t, Ru–H); 7.24–7.82 (m, PPh_3); 8.29 (d, pyrazine); 8.73 (d, pyrazine). ^{31}P NMR (δ, $CDCl_3$): 45.64 (s, PPh_3). UV–Vis [nm] in CH_2Cl_2 (log ε): 418.4 (3.11); 381.1 sh (3.19); 260.0 (3.81); 223.2 (4.31); 216.4 (4.10).

2.3. *DFT calculations*

Gaussian-03 [15] was used for the calculations. The geometry optimisation was carried out using the DFT method with the B3LYP functional [16, 17]. Electronic transitions were calculated with the PCM model [18] in dichloromethane solution. The calculation was performed using the DZVP basis set [19] with *f* functions with exponents 1.94722036 and 0.748930908 on ruthenium, and polarization functions for all other atoms: 6-31 g(2d,p) – chlorine, 6-31 g** – carbon, nitrogen, oxygen, and 6-31 g(d,p) – hydrogen. Natural bond orbital (NBO) calculations were performed using the NBO code [20] included in Gaussian 03.

2.4. *Crystal structure determination and refinement*

A yellow needle of $[RuHCl(CO)(PPh_3)_2(C_4H_4N_2)]$ was mounted on a KM-4-CCD automatic diffractometer equipped with CCD detector, used for data collection.

X-ray intensity data were collected with graphite monochromated Mo-Kα radiation ($\lambda = 0.71073$ Å) at 291.0(3) K, with ω scan mode. The full Ewald sphere reflections were collected up to $2\theta = 50.1^\circ$. Unit cell parameters were determined based on least-squares refinement of the setting angles of 7268 strongest reflections. Details concerning crystal data and refinement are given in table 1. During the data reduction above, a decay correction coefficient was taken into account. Lorentz, polarization, and numerical absorption [21] corrections were applied. The structure was solved by direct methods. All the non-hydrogen atoms were refined anisotropically using full-matrix, least-squares techniques on F^2. The carbon bonded hydrogen atoms were found from difference Fourier synthesis after four cycles of anisotropic refinement, and refined as "riding" on the adjacent atom with individual isotropic temperature factor 1.2 times the value of the equivalent temperature factor of the parent atom. The H(1R) atom was placed in calculated position (Re–H distance 1.6 Å) according to similar structures [22]. SHELXS97 [23], SHELXL97 [24] and SHELXTL [25] programs were used for all calculations. Atomic scattering factors had values incorporated in the computer programs.

3. Results and discussion

Reaction between $[RuHCl(CO)(PPh_3)_3]$ and pyrazine in methanolic solution yields the mononuclear ruthenium(II) compound $[RuHCl(CO)(pz)(PPh_3)_2]$ (pz = pyrazine) as a yellow, air-stable, crystalline solid. Infrared spectrum of the complex exhibits

Table 1. Crystal data and structure refinement details of $[RuHCl(CO)(pyrazine)(PPh_3)_2] \cdot 0.5CH_3OH$.

Empirical formula	$C_{83}H_{74}Cl_2N_4O_3P_4Ru_2$
Formula weight	1572.38
Temperature (K)	291.0(3)
Crystal system	Monoclinic
Space group	$P2_1/c$
Unit cell dimensions (Å, °)	
a	20.8661(15)
b	14.7041(11)
c	25.154(2)
β	102.554(7)
Volume (Å^3)	7533.2(10)
Z	4
Calculated density (Mg m^{-3})	1.386
Absorption coefficient (mm^{-1})	0.608
$F(000)$	3224
Crystal dimensions (mm^3)	$0.498 \times 0.221 \times 0.220$
θ range for data collection (°)	2.83–25.13
Index ranges	$-24 \le h \le 24$, $-17 \le k \le 17$, $-26 \le l \le 30$
Reflections collected	78342
Independent reflections	13412 [$R_{(int)} = 0.0907$]
Data/restraints/parameters	13412/0/885
Goodness-of-fit on F^2	1.084
Final R indices [$I > 2\sigma(I)$]	$R_1 = 0.0680$, $wR_2 = 0.1707$
R indices (all data)	$R_1 = 0.0923$, $wR_2 = 0.1894$
Largest diff. peak and hole (e Å^{-3})	1.002 and −1.413

characteristic bands due to coordinated ligands – pyrazine, CO, PPh_3 and hydride group. The strong band at 1932 cm^{-1} is assigned to the ν_{CO} of carbonyl bonded to ruthenium, and the band at 2005 cm^{-1} corresponds to ν_{Ru-H}. The ν_{CO} and ν_{Ru-H} stretching bands in the parent $[RuHCl(CO)(PPh_3)_3]$ complex are at 2020 and 1903 cm^{-1} respectively. The band at 1586 cm^{-1} is attributed to the CN stretch of pyrazine present in the complex. The positions of the ν_{CO} and ν_{Ru-H} bands in the IR spectrum of the complex indicate a decrease in the metal – carbonyl carbon interaction and an increase in the Ru–H bond order.

The ^1H NMR contains a triplet at −13.55 ppm, resulting from hydrido ligand. The pyrazine and triphenylphosphine ligands give signals at 8.29, 8.73 and 7.24–7.82 ppm respectively. The singlet at 45.64 ppm in the ^{31}P NMR spectrum indicated both the triphenylphosphoine ligands in the studied complex are equivalent and mutually *trans*.

3.1. *Crystal structure*

The $[RuHCl(CO)(pz)(PPh_3)_2]$ complex crystallizes in the monoclinic space group $P2_1/c$. The relative orientation of molecules is depicted in figure 1, which also shows displacement ellipsoids (structure of the complex is presented in figure 2). The selected bond lengths and angles are listed in table 2. The two crystallographically independent molecules are structurally nearly identical (I and II hereafter for molecules containing Ru(1) and Ru(51) respectively). The most different distances are Ru(1)–P(1) 2.366(13) Å and Ru(51)–P(51) 2.353(13) Å. The most different angles are P(2)–Ru(1)–Cl(1) 93.57(4)° and P(52)–Ru(51)–Cl(51) 97.20(4)°, C(41)–Ru(1)–Cl(1) 97.72(16)° and

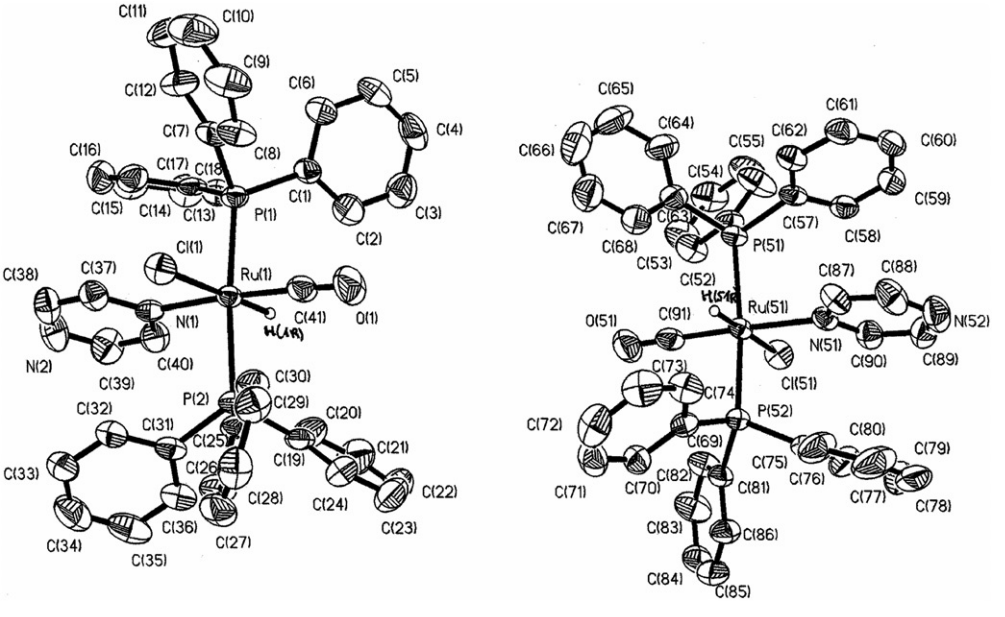

Figure 1. Relative orientation of two molecules of $[RuHCl(CO)(pyrazine)(PPh_3)_2]$ in the asymmetric unit. The displacement ellipsoids are drawn with 50% probability. The solvent molecule was omitted for clarity.

C(91)–Ru(51)–Cl(51) 94.98(16)°, P(1)–Ru(1)–P(2) 172.96(4)° and P(51)–Ru(51)–P(52) 170.49(4)°. The ruthenium atom is in a distorted octahedral environment with CO *trans* to pyrazine ligand, two mutually *trans* PPh_3 ligands and the Cl and hydrido ligands *trans*. The Ru–Cl bond distances (2.518(12)–2.503(12) Å) are longer than the ones reported in the literature for Ru^{II} complexes due to the *trans* effect of hydride [26]. The pyrazine and triphenylphosphine ligands display normal distances. The solvent molecule shows of disorder. A careful inspection of difference electron density maps did not show any local minima/maxima, thus one may suppose that the disorder has dynamical character. One intermolecular interaction which can be classified as O(99)–H(99)···N(52) hydrogen bond (D···A distance 2.899(5) Å, H···A distance 2.21 Å, and D–H···A angle 141°) is found in the structure.

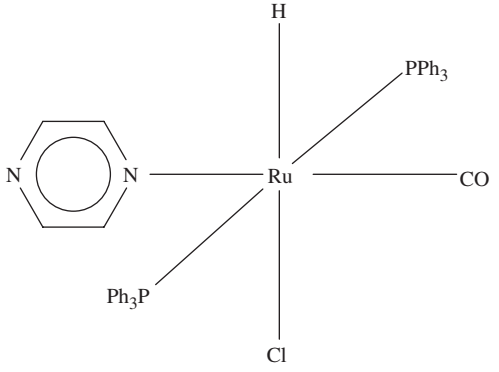

Figure 2. Structural drawing of [RuHCl(CO)(pyrazine)$(PPh_3)_2$].

Table 2. Selected bond lengths (Å) and angles (°) for [RuHCl(CO)(pyrazine)$(PPh_3)_2$].

Experimental				Calculated
Ru(1)–C(41)	1.830(5)	Ru(51)–C(91)	1.836(5)	1.855
Ru(1)–N(1)	2.193(4)	Ru(51)–N(51)	2.201(4)	2.266
Ru(1)–P(1)	2.366(13)	Ru(51)–P(51)	2.353(13)	2.431
Ru(1)–P(2)	2.378(13)	Ru(51)–P(52)	2.365(13)	2.434
Ru(1)–Cl(1)	2.518(12)	Ru(51)–Cl(51)	2.503(12)	2.576
Ru(1)–H(1R)	1.600	Ru(51)–H(51R)	1.600	1.609
C(41)–Ru(1)–N(1)	173.39(19)	C(91)–Ru(51)–N(51)	174.67(17)	170.88
C(41)–Ru(1)–P(1)	90.63(15)	C(91)–Ru(51)–P(51)	90.25(15)	88.69
N(1)–Ru(1)–P(1)	90.53(10)	N(51)–Ru(51)–P(51)	92.73(10)	91.52
C(41)–Ru(1)–P(2)	87.46(15)	C(91)–Ru(51)–P(52)	87.12(15)	88.56
N(1)–Ru(1)–P(2)	90.60(10)	N(51)–Ru(51)–P(52)	89.24(10)	90.80
P(1)–Ru(1)–P(2)	172.96(4)	P(51)–Ru(51)–P(52)	170.49(4)	176.29
C(41)–Ru(1)–Cl(1)	97.72(16)	C(91)–Ru(51)–Cl(51)	94.98(16)	100.80
N(1)–Ru(1)–Cl(1)	88.71(10)	N(51)–Ru(51)–Cl(51)	89.32(10)	88.31
P(1)–Ru(1)–Cl(1)	93.40(4)	P(51)–Ru(51)–Cl(51)	92.12(4)	90.86
P(2)–Ru(1)–Cl(1)	93.57(4)	P(52)–Ru(51)–Cl(51)	97.20(4)	92.10
C(41)–Ru(1)–H(1R)	82.3	C(91)–Ru(51)–H(51R)	82.8	89.67
P(1)–Ru(1)–H(1R)	86.6	P(52)–Ru(51)–H(51R)	85.0	86.19
P(2)–Ru(1)–H(1R)	86.4	P(51)–Ru(51)–H(51R)	87.9	87.66
N(1)–Ru(1)–H(1R)	91.3	N(51)–Ru(51)–H(51R)	90.7	84.70
Cl(1)–Ru(1)–H(1R)	180.0	Cl(51)–Ru(51)–H(51R)	180.0	173.00

3.2. *Optimized geometries*

The geometry of the studied complex was optimized in singlet states using the DFT method with the B3LYP functional. The optimized geometric parameters of the singlet state of the complex are gathered in table 2. In general, the predicted bond lengths and angles are in good agreement with the values based on the X-ray crystal structure data, and the general trends observed in the experimental data are well reproduced in the calculations. The largest differences are observed in the Ru–N and ruthenium–phosphine distances: 0.0715 and 0.069 Å, respectively. Maximum deviation between the calculated angles and the average observed ones is close to 7.12° (carbonyl–ruthenium–hydride).

3.3. *Electronic structure and NBO analysis*

The bonding of CO to the ruthenium center involves a synergic interaction between the carbonyl ligand orbitals and the metal orbitals. The Ru–CO bond consists of two components (i) a donation of electron density from a σ-type orbital of CO onto the metal orbital and (ii) a donation of electron density from the occupied metal d-orbitals onto the π^* anti-bonding orbitals of the CO ligand. In the studied complex, the occupied d_{xy} and d_{xz} ruthenium orbitals participate in the back donation from ruthenium to carbonyl. The largest contribution of the π_{Ru-CO} bonding interaction is visible in the HOMO, H-1 and H-5 orbitals. The π^*_{Ru-CO} orbitals are also distributed among several unoccupied molecular orbitals. Their contribution is visible in L + 14, L + 15 and L + 17 orbitals. The HOMO orbital of $[RuHCl(CO)(pz)(PPh_3)_2]$ is composed of the d_{xz} metal orbital and chlorine π orbital in anti-bonding arrangement. The LUMO is localized on the pyrazine ring. The d_{z^2} orbital of Ru atom makes the largest contribution into L + 2 and, L + 14 and L + 17 have $d_{x^2-y^2}$ character. Figure 3 presents the molecular orbitals of the studied complex, in which the interaction between ruthenium ion and carbonyl, phosphorus or hydride ligands is visible.

In some of the lowest unoccupied molecular orbitals of $[RuHCl(CO)(pz)(PPh_3)_2]$, the contribution of the phosphorus orbitals is visible (see figure 3). In classical concepts empty phosphorous 3d orbitals are used in π-back bonding between metal center and phosphine ligand. It is generally recognized that the d orbitals have very high energy and play only a minor role in the π_{M-PR3} bond formation [27]. In the π-back bonding between metal center and phosphine ligand, the σ^*(P–C) orbitals are involved. The HOMO–LUMO gap is 3.59 eV.

The energy and character of selected frontier molecular orbitals are given in table 4. The ruthenium–hydride ligand interaction is visible in the H-4, H-7 and L + 14, L + 17 molecular orbitals.

The natural bond orbital (NBO) σ_{AB} can be written in terms of two directed valence hybrids (HHOs) h_A and h_B on atoms A and B:

$$\sigma^*_{AB} = c_A h_A + c_B h_B$$

where c_A and c_B are polarization coefficients. Each valence bonding NBO must in turn be paired with a corresponding valence *anti*-bonding NBO:

$$\sigma^*_{AB} = c_B h_A - c_A h_B$$

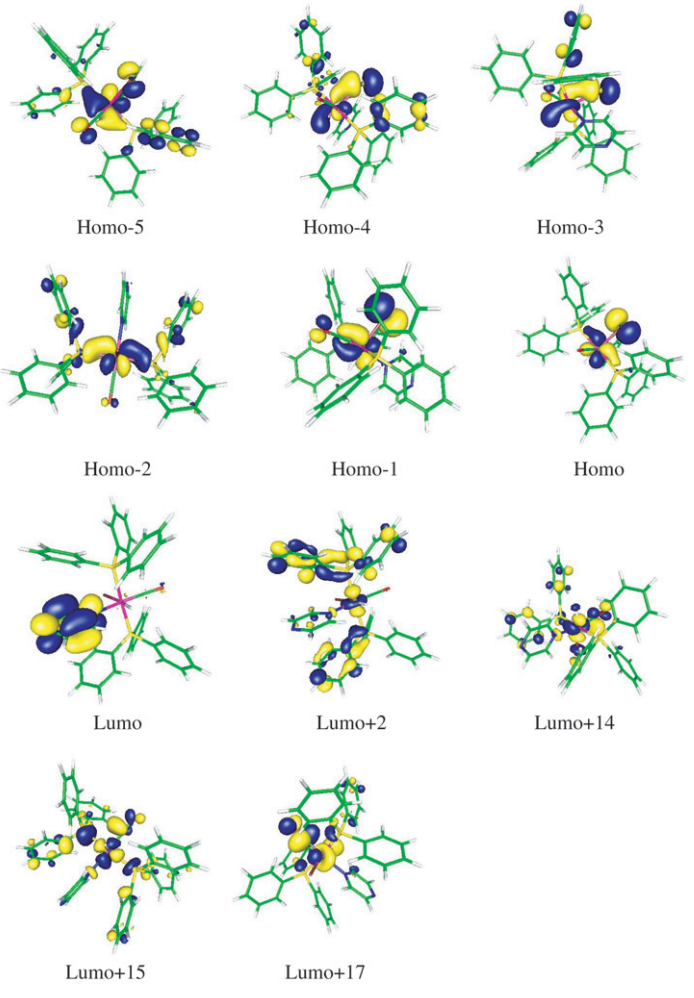

Figure 3. Contours of several HOMO and LUMO molecular orbitals of [RuHCl(CO)(pyrazine)(PPh_3)$_2$].

Table 3. The occupancies and hybridization of the calculated Ru–C and C–O natural bond orbitals (NBOs) for [RuHCl(CO)(pyrazine)(PPh_3)$_2$].

BD (2-center bond)	Occupancy	Hybridization of NBO
Ru(1)–C(48)	1.935 (0.269)	$0.564(sd^{2.34})_{Ru} + 0.838(sp^{0.54})_C$
C(1)–O(1)	1.994 (0.014)	$0.553(sp^{1.88})_C + 0.833(sp^{1.15})_O$
	1.996 (0.229)	$0.496(p)_C + 0.869(p)_O$
	1.997 (0.247)	$0.492(p)_C + 0.871(p)_O$

to complete the span of the valence space. The Lewis-type (donor) NBOs are thereby complemented by non-Lewis-type (acceptor) NBOs that are formally empty in an idealized Lewis picture. Interactions between 'filled' Lewis-type NBOs and 'empty' non-Lewis NBOs lead to loss of occupancy from the localized NBOs of the idealized Lewis

Table 4. Energy and character of selected MOs of [RuHCl(CO)(pyrazine)(PPh_3)$_2$].

MO	Energy (eV)	Character
H-17	−7.329	π_{Ph}
H-16	−7.192	$d_{Ru}+\pi_{Cl}+\pi_{Ph}$
H-15	−7.150	π_{Ph}
H-14	−7.067	$d_{Ru}+\pi_{Cl}+\pi_{Ph}$
H-13	−6.977	π_{Ph}
H-12	−6.954	π_{Ph}
H-11	−6.904	π_{Ph}
H-10	−6.870	π_{Ph}
H-9	−6.843	π_{Ph}
H-8	−6.769	π_{Ph}
H-7	−6.740	$d_{Ru}+\sigma_{Cl}+\sigma_{H}$
H-6	−6.690	π_{Ph}
H-5	−6.634	$d_{Ru}+\pi_{Cl}+\pi_{CO}$
H-4	−6.565	$d_{Ru}+\sigma_{Cl}+\sigma_{H}$
H-3	−6.444	$d_{Ru}+\sigma_{Cl}+\sigma_{H}$
H-2	−6.184	$d_{Ru}+np$
H-1	−5.692	$d_{Ru}+\pi^*_{Cl}+\pi^*_{CO}$
Homo	−5.419	$d_{Ru}+\pi^*_{Cl}+\pi^*_{CO}$
Lumo	−1.826	π^*_{pz}
L+1	−0.935	$\pi^*_{pz}+\pi^*_{Ph}$
L+2	−0.689	$d_{Ru}+\pi^*_{Ph}$
L+3	−0.574	$\pi^*_{Ph}+n_P$
L+4	−0.508	$\pi^*_{Ph}+n_P$
L+5	−0.449	π^*_{Ph}
L+6	−0.347	π^*_{Ph}
L+7	−0.254	π^*_{Ph}
L+8	−0.148	π^*_{Ph}
L+9	−0.119	π^*_{Ph}
L+10	0.005	π^*_{Ph}
L+11	0.071	π^*_{Ph}
L+12	0.143	π^*_{Ph}
L+13	0.167	π^*_{Ph}
L+14	0.356	$d_{Ru}+\pi^*_{CO}+\sigma^*_{Cl}$
L+15	0.806	$d_{Ru}+\pi^*_{CO}-n_P$
L+16	0.963	$d_{Ru}+\pi^*_{CO}$
L+17	1.248	$d_{Ru}+\pi^*_{CO}-\sigma_{H}$

structure into the empty non-Lewis orbitals, and they are referred to as 'delocalization' corrections to the zeroth-order natural Lewis structure.

The occupancy and hybridization of the calculated natural bond orbital (NBO) between the ruthenium and the hydrido ligand is 1.849 and $0.6934(sd^{2.54})_{Ru}+0.721(s)_H$ respectively; the occupancy of the antibonding orbital of Ru–H is 0.271.

For the carbonyl group, three natural bond orbitals were detected for the C–O bond, and one for the Ru–C bond. The Ru–C bond orbitals are polarized towards the carbon atom, and the C–O bond orbitals are polarized towards the oxygen. The oxygen of the carbonyl ligand has one lone pair (LP) orbital. The occupancies and hybridization of the CO and Ru–C bonds are gathered in table 3 (*anti*-bonding NBOs are given in round brackets).

Not detected in NBO analysis Ru–N_{pz} bonds have character of predominant Coulomb-type interactions between the central ion and pyrazine ligand [28].

The resonance structure $M{-}\overset{+}{C}{\equiv}O{:}$, which presents the bonding between CO ligands and Ru ion in [RuHCl(CO)(pz)(PPh_3)$_2$], is consistent with the values of the

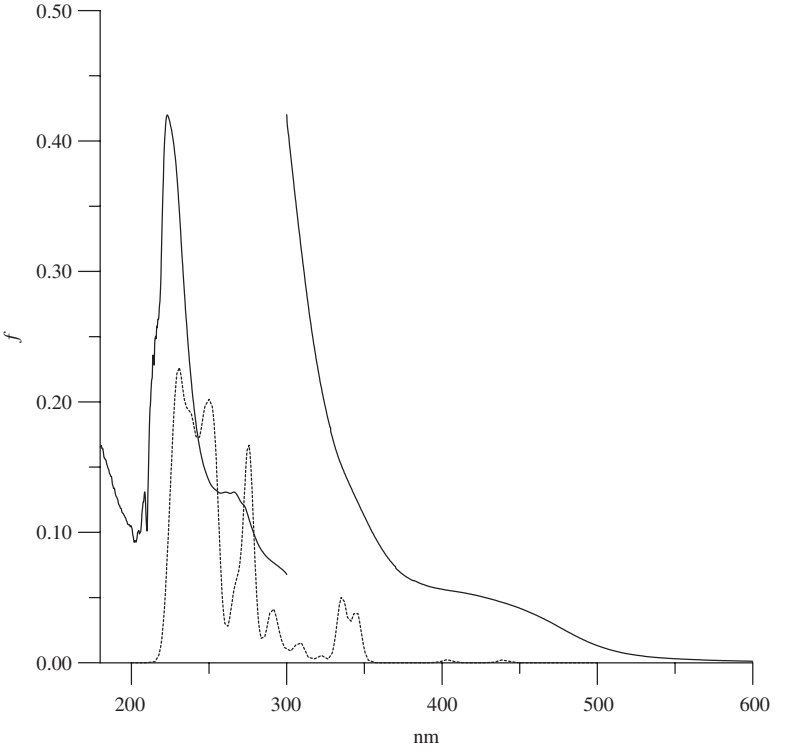

Figure 4. The UV–Vis spectra of [RuHCl(CO)(pyrazine)(PPh_3)$_2$] (solid line – experimental; dashed line – calculated).

calculated atomic charges. The calculated charge on the ruthenium atom of the complex is close to 0 with negative sign (−0.094); formally ruthenium is +2. The charge on the carbon atom of the carbonyl ligand is positive (+0.576), whereas the oxygen atom is negatively charged (−0.499). The charge of hydride ligand is close to −0.093. The occupancies of the ruthenium d orbitals, obtained from NBO analysis, are: d_{xy} – 1.73; d_{xz} – 1.93; d_{yz} – 1.76; d_{z^2} – 1.22; $d_{x^2-y^2}$ – 1.06. The nitrogen donor atom of pyrazine has −0.45 charge and the second −0.41. The occupancies of the lone pairs in the N-pyrazine atoms are 1.79 and 1.93 the bound and unbound nitrogens respectively.

3.4. *Electronic spectrum*

The experimental and calculated electronic spectra of [RuHCl(CO)(pz)(PPh_3)$_2$] are presented in figure 4. Each calculated transition is represented by a Gaussian function $y = ce^{-bx^2}$ with the height (c) equal to the oscillator strength and b equal to 0.04 nm^{-2}. 90 electronic transitions were calculated using the TDDFT method and they do not comprise all the experimental absorption bands. The UV–Vis spectrum was calculated up to ~225 nm, so the shortest wavelength experimental bands cannot be assigned to calculated transitions. However, considering that the solution spectra of PPh_3 and pyrazine exhibit intense absorption bands in the 260–200 nm region, some additional intraligand and interligand transitions are expected to be found at higher energies in the calculations.

The assignments of calculated transitions to experimental bands are based on the criterion of the energy and oscillator strength of the calculated transitions. In the description of the electronic transitions only the main components of the molecular orbital are taken into consideration.

The longest wavelength experimental broad band with maximum at 418.2 nm is assigned to the transitions from HOMO-1 and HOMO to LUMO orbitals. As the LUMO orbital is composed of the π^* orbitals of the pyrazine ring, the transition is of *Metal–Ligand Charge Transfer* type.

The shoulder (może "hump"?) at 381.1 nm results from transitions from HOMO to LUMO + 1 and LUMO + 2 MOs. These transitions are excitations from central metal d orbitals to the π^* orbitals of pyrazine ligand and $d \rightarrow d$ (LF).

The asymmetric band with maximum at 260.0 nm is ascribed to the metal–ligand charge transfer transitions ($d \rightarrow \pi^*_{pz}$ and $d \rightarrow \pi^*_{ph}$) with a mixture of *Ligand–Ligand Charge Transfer* transitions ($\pi_{Ph} \rightarrow \pi^*_{pz}$). The last calculated transition attributed to the experimental one at 223.2 nm proceeds mainly from the d ruthenium orbitals with admixture of π chloride and π carbonyl orbitals to π^*_{ph} and π^*_{pz}.

The experimental band at 216.4 nm could not be assigned on the basis of the calculated transitions; it can be assumed that the band results from transitions in the PPh_3 ligands and from $\pi \rightarrow \pi^*$ excitations in the pyrazine ligand.

Supplementary material

More details of the crystal structure determinations have been deposited with the Cambridge Crystallographic Data Centre with the deposition number: CCDC 615581.

Acknowledgements

Crystallographic part was financed by funds allocated by Ministry of Science and Higher Education to the X-ray Crystallography and Crystal Chemistry Group, Institute of General and Ecological Chemistry, Technical University of Łódź. The Gaussian 03 calculations were carried out in the Wrocław Centre for Networking and Supercomputing, WCSS, Wrocław, Poland under calculational grant No. 51/96.

References

[1] E. Iengo, G. Mestroni, S. Geremia, M. Calligaris, E. Alessio. *J. Chem. Soc., Dalton Trans.*, 3361 (1999).
[2] E. Iengo, E. Zangrando, S. Mestroni, G. Fronzoni, M. Stener, E. Alessio. *J. Chem. Soc., Dalton Trans.*, 1338 (2001).
[3] B. Serli, E. Iengo, T. Gianferrara, E. Zangrando, E. Alessio. *Met. Based Drugs*, **8**, 9 (2001).
[4] B. Serli, E. Zangrando, E. Iengo, E. Alessio. *Inorg. Chim. Acta*, **339**, 265 (2002).
[5] C. Dragonetti, M. Pizzotti, D. Roberto, S. Galli. *Inorg. Chim. Acta*, **330**, 128 (2002).
[6] D. Brown, S. Muranjan, R.P. Thummel. *Eur. J. Inorg. Chem.*, **19**, 3547 (2003).

[7] H. Casey, C.P. Kubiack. *J. Phys. Chem. A*, **107**, 9301 (2003).
[8] T. Yamaguchi, N. Imai, T. Ito, C.P. Kubiak. *Bull. Chem. Soc. Jpn*, **73**, 1205 (2000).
[9] C. Londergan, R. Rocha, M.C. Brown, A.P. Shreve, C.P. Kubiack. *J. Am. Chem. Soc.*, **125**, 13912 (2003).
[10] Z. Fang, S. Swavey, A. Holder, B. Winkel, K.J. Brewer. *Inorg. Chem. Commun.*, **5**, 1078 (2002).
[11] L. Alvila, T.A. Pakkanen. *J. Mol. Cat.*, **84**, 145 (1993).
[12] D. Bianchi, M. Bertoli, R. Tassinari, M. Ricci, M. Vignola. *J. Mol. Cat. A: Chem.*, **200**, 111 (2003).
[13] H. Chermette. *Coord. Chem. Rev.*, **178–180**, 699 (1998).
[14] N. Ahmad, J.J. Levinson, S.D. Robinson, M.F. Uttely. *Inorg. Synth.*, **15**, 48 (1974).
[15] M.J. Frisch, G.W. Trucks, H.B. Schlegel, G.E. Scuseria, M.A. Robb, J.R. Cheeseman, J.A. Montgomery, Jr., T. Vreven, K.N. Kudin, J.C. Burant, J.M. Millam, S.S. Iyengar, J. Tomasi, V. Barone, B. Mennucci, M. Cossi, G. Scalmani, N. Rega, G.A. Petersson, H. Nakatsuji, M. Hada, M. Ehara, K. Toyota, R. Fukuda, J. Hasegawa, M. Ishida, T. Nakajima, Y. Honda, O. Kitao, H. Nakai, M. Klene, X. Li, J.E. Knox, H.P. Hratchian, J.B. Cross, C. Adamo, J. Jaramillo, R. Gomperts, R.E. Stratmann, O. Yazyev, A.J. Austin, R. Cammi, C. Pomelli, J.W. Ochterski, P.Y. Ayala, K. Morokuma, G.A. Voth, P. Salvador, J.J. Dannenberg, V.G. Zakrzewski, S. Dapprich, A.D. Daniels, M.C. Strain, O. Farkas, D.K. Malick, A.D. Rabuck, K. Raghavachari, J.B. Foresman, J.V. Ortiz, Q. Cui, A.G. Baboul, S. Clifford, J. Cioslowski, B.B. Stefanov, G. Liu, A. Liashenko, P. Piskorz, I. Komaromi, R.L. Martin, D.J. Fox, T. Keith, M.A. Al-Laham, C.Y. Peng, A. Nanayakkara, M. Challacombe, P.M.W. Gill, B. Johnson, W. Chen, M.W. Wong, C. Gonzalez, J.A. Pople. *Gaussian 03, Revision B.03*, Gaussian, Inc., Pittsburgh PA (2003).
[16] A.D. Becke. *J. Chem. Phys.*, **98**, 5648 (1993).
[17] C. Lee, W. Yang, R.G. Parr. *Phys. Rev. B*, **37**, 785 (1988).
[18] B. Mennucci, J. Tomasi. *J. Chem. Phys.*, **106**, 5151 (1997).
[19] K. Eichkorn, F. Weigend, O. Treutler, R. Ahlrichs. *Theor. Chim. Acc.*, **97**, 119 (1997).
[20] E.D. Glendening, A.E. Reed, J.E. Carpenter, F. Weinhold. NBO (version 3.1).
[21] A.D. Becke. *J. Chem. Phys.*, **98**, 5648 (1993).
[22] M.V. Ovchinnikov, A.M. Ellern, I.A. Guzei, R.J. Angelici. *Inorg. Chem.*, **40**, 7014 (2001); S.M. Boniface, G.R. Clark, T.J. Collins, W.R. Roper. *J. Organomet. Chem.*, **206**, 109 (1981); H. Werner, W. Stuer, B. Weberndorfer. *J. Wolf. Eur. J. Inorg. Chem.*, **10**, 1707 (1999); P.C. Junk, J.W. Steed. *J. Organomet. Chem.*, **587**, 191 (1999); A. Romero, A. Vegas, A. Santos, A.M. Cuadro. *J. Chem. Soc., Dalton Trans.*, 183 (1987); J.G. Haasnoot, W. Hinrichs, O. Weir, J.G. Vos. *Inorg. Chem.*, **25**, 4140 (1986); E. Bonfada, C. Maichle-Mossmer, J. Strahle, U. Abram. *Z. Anorg. Allg. Chem.*, **625**, 1327 (1999).
[23] G.M. Sheldrick. *Acta Cryst.*, **A46**, 467 (1990).
[24] G.M. Sheldrick. *SHELXL97. Program for the Solution and Refinement of Crystal Structures*. University of Göttingen, Germany (1997).
[25] G.M. Sheldrick. *SHELXTL*. Release 4.1 for Siemens Crystallographic Research Systems (1990).
[26] M.A. Moreno, M. Haukka, A. Turunen, T.A. Pakkanen. *J. Mol. Catal. A*, **240**, 7 (2005); B. Serli, E. Zangrando, E. Iengo, E. Alessio. *Inorg. Chim. Acta*, **339**, 265 (2002).
[27] A. Vogler, H. Kunkely. *Coord. Chem. Rev.*, **230**, 243 (2002).
[28] L. Kuznestov, A.J.L. Pombeiro. *J. Chem. Soc., Dalton Trans.*, 738 (2003).